Journal of Cerebral Blood Flow & Metabolism (2014) 34, 708–714

www.jcbfm.com

ORIGINAL ARTICLE

PET imaging of ischemia-induced impairment of mitochondrial complex I function in monkey brain

Hideo Tsukada, Hiroyuki Ohba, Shingo Nishiyama, Masakatsu Kanazawa, Takeharu Kakiuchi and Norihiro Harada

To assess the capability of ^{18}F-2-tert-butyl-4-chloro-5-{6-[2-(2-fluoroethoxy)-ethoxy]-pyridin-3-ylmethoxy}-2H-pyridazin-3-one (^{18}F-BCPP-EF), a novel positron emission tomography (PET) probe for mitochondrial complex I (MC-I) activity, as a specific marker of ischemia-induced neuronal death without being disturbed by inflammation, translational research was conducted using an animal PET in ischemic brains of Cynomolgus monkeys (*Macaca fascicularis*). Focal ischemia was induced by the right middle cerebral artery occlusion for 3 hours, then PET scans were conducted at Day-7 with ^{15}O-gases for regional cerebral blood flow (rCBF) and regional cerebral metabolism of oxygen ($rCMRO_2$), and ^{18}F-BCPP-EF for MC-I with arterial blood sampling. On Day-8, the additional PET scans conducted with ^{11}C-flumazenil (^{11}C-FMZ) for central-type benzodiazepine receptors, ^{11}C-PBR28 for translocator protein, and ^{18}F-fluoro-2-deoxy-D-glucose (^{18}F-FDG) for regional cerebral metabolic rate of glucose (rCMRglc). The total distribution volume (V_T) values of ^{18}F-BCPP-EF showed the significant reduction in MC-I activity in the damaged area at Day-7. When correlated with rCBF and $rCMRO_2$, the V_T values of ^{18}F-BCPP-EF provided better correlation with $rCMRO_2$ than with rCBF. In the inflammatory regions (region of interest, ROI_{PBR}) of the ischemic hemisphere detected with ^{11}C-PBR28, higher ^{18}F-FDG uptake and lower V_T of ^{18}F-BCPP-EF, ^{11}C-FMZ, and $rCMRO_2$ than those in normal contralateral hemisphere were observed. These results strongly suggested that ^{18}F-BCPP-EF could discriminate the neuronal damaged areas with neuroinflammation, where ^{18}F-FDG could not owing to its high uptake into the activated microglia.

Journal of Cerebral Blood Flow & Metabolism (2014) **34,** 708–714; doi:10.1038/jcbfm.2014.5; published online 22 January 2014

Keywords: brain imaging; ischemia; mitochondria; microglia; molecular imaging

INTRODUCTION

The mitochondrial respiratory chain (complexes I to V) is the major site of ATP production in eukaryotes. This organelle not only generates ATP, but also has an important role in the center of the apoptotic signaling pathway.[1] Among these five complexes, mitochondrial complex I (MC-I; NADH–ubiquinone oxidoreductase, EC 1.6.5.3) is the first enzyme of the respiratory electron transport chain. MC-I takes two electrons from NADH and transfers them to ubiquinone in the inner-mitochondrial membrane. Mitochondrial complex I uses the energy released from this process to move four protons across the membrane, creating charge separation across the membrane.

Mitochondrial dysfunction contributes to the pathophysiology of acute neurologic disorders and neurodegenerative diseases.[2] Mitochondria are considered the main intracellular source of reactive oxygen species (ROS) in cells and also the main target of ROS-mediated damage. Ischemia may cause mitochondrial alterations that would favor ROS production when the oxygen concentration is reestablished by reperfusion.[3] We showed that, immediately after reperfusion from the middle cerebral artery (MCA) occlusion (MCAO) for 3 hours (3-hour MCAO), postischemic hyperperfusion was observed in the neocortical area of monkey brain.[4,5] When ischemic tissue is reoxygenated, electron transport through the respiratory chain is impaired because of depletion of ADP during ischemia, and this leads to a burst of ROS generation during the first minutes of reoxygenation.[3]

To image MC-I function in the living brain using positron emission tomography (PET), we recently synthesized several novel PET probes,[6] and confirmed that ^{18}F-2-tert-butyl-4-chloro-5-{6-[2-(2-fluoroethoxy)-ethoxy]-pyridin-3-ylmethoxy}-2H-pyridazin-3-one (^{18}F-BCPP-EF) was most preferable for MC-I imaging in the living brain of rat[6,7] and monkey.[8] Since whole-body PET imaging of rat indicated relatively high uptake and long retention in the brain,[6,7] we hypothesized that PET probes for MC-I could be applicable for the imaging of neuronal damage in living brain. It was suggesting that ^{18}F-BCPP-EF could be useful to detect ischemic neuronal damage at the subacute phase 7 days after ischemic insult (Day-7),[7] at which time unexpectedly higher ^{18}F-fluoro-2-deoxy-D-glucose (FDG) uptake was observed in the damaged area than in the contralateral intact area.[9,10] The FDG-PET is a well-established technique for quantitative imaging of the regional cerebral metabolic rate of glucose (rCMRglc) in living brain, which is based on the assumption that rCMRglc reflects energy metabolism *via* oxidative phosphorylation. However, the unexpectedly high uptake of ^{18}F-FDG in ischemia-damaged areas suggested that ^{18}F-FDG was taken up into not only normal tissues but also inflammatory regions with microglial activation.[9,10] Since recent PET research has indicated that neurodegenerative disorders showed neuroinflammation with microglial activation,[11] PET probes to image MC-I activity would be favorable for more accurate assessment of neurodegenerative damage using PET.

The present study aimed to validate ^{18}F-BCPP-EF, a novel PET probe for MC-I activity, as a specific marker of ischemia-induced neuronal death without being disturbed by inflammation. The binding properties of ^{18}F-BCPP-EF were assessed in an ischemic brain model of living monkey using high-resolution PET, and its

Central Research Laboratory, Hamamatsu Photonics K.K., Shizuoka, Japan. Correspondence: Dr H Tsukada, Central Research Laboratory, Hamamatsu Photonics K.K., 5000 Hirakuchi, Hamakita, Shizuoka 434-8601, Japan.
E-mail: tsukada@crl.hpk.co.jp
Received 7 November 2013; revised 26 December 2013; accepted 2 January 2014; published online 22 January 2014

cerebral uptake was compared with the regional cerebral blood flow (rCBF), regional cerebral metabolism of oxygen ($rCMRO_2$) measured with ^{15}O-gases, ^{11}C-flumazenil (^{11}C-FMZ) binding to the central-type benzodiazepine receptor (CBR), ^{11}C-PBR28 binding to the translocator protein, and regional cerebral blood flow (rCMRglc) measured with ^{18}F-FDG at Day-7/8 after 3-hour MCAO ischemic insult in the monkey brain.

MATERIALS AND METHODS

Animals and Drugs

Animals were maintained and handled in accordance with the recommendations of the US National Institutes of Health and the guidelines of the Central Research Laboratory, Hamamatsu Photonics. The following experiments were approved by the Ethical Committee of the Central Research Laboratory, Hamamatsu Photonics. Seven male Cynomolgus monkeys (*Macaca fascicularis*) at the age between 4.5 and 5.3 years old with body weights ranging from 4.5 to 5.8 kg were used for the PET measurements. Magnetic resonance (MR) images (MRIs) of the monkeys were obtained with a 3.0-T MR imager (Signa Excite HDxt 3.0T; GE Healthcare Japan, Tokyo, Japan) using a 3D-Spoiled Gradient Echo sequence (176 slices with a 256×256 image matrix, slice thickness/spacing of 1.4/0.7 mm, echo time: 3.4 to 3.6 ms, repetition time: 7.7 to 8.0 ms, inversion time: 400 ms, and flip angle, 15°) under pentobarbital anesthesia. We could not conduct MR imaging after ischemic insult because our MRI system was located outside the radiation regulated area. Japanese low for the radiation safety regulation did not allow us to bring out the animals injected even positron emitters with short half-lives from radiation regulated area.

Isoflurane and pancronium were purchased from Dainippon Pharmaceutical (Osaka, Japan) and Sankyo Co. Ltd. (Tokyo, Japan), respectively. Rabbit anti-Iba1 polyclonal antibody was from Wako Pure Chemical Industry (Osaka, Japan). Mouse anti-NeuN monoclonal antibody and EnVision were obtained from Millipore (Billerica, MA, USA) and DAKO (Carpinteria, CA, USA), respectively. Precursors of ^{18}F-BCPP-EF, ^{11}C-FMZ, and ^{11}C-PBR28, and their corresponding cold compounds, were purchased from NARD Institute (Amagasaki, Japan). Mannose triflate and Kryptofix222 (K[2,2,2]) were obtained from ABX (Radeberg, Germany) and Merck (Darmstadt, Germany), respectively.

Positron Emission Tomography Ligand Syntheses

Positron-emitting carbon-11 (^{11}C), oxygen-15 (^{15}O), and fluorine-18 (^{18}F) were produced by ^{14}N(p, α)^{11}C, ^{14}N(d, n)^{15}O, and ^{18}O(p, n)^{18}F nuclear reactions, respectively, using a cyclotron (HM-18; Sumitomo Heavy Industry, Tokyo, Japan) at Hamamatsu Photonics PET Center. Labeled compounds were synthesized using a modified CUPID system (Sumitomo Heavy Industries, Ltd., Tokyo, Japan). HPLC analyses of labeled compounds were performed on a GL-7400 low-pressure gradient HPLC system (GL Sciences, Inc., Tokyo, Japan) with a radioactivity detector (RLC-700; Hitachi Aloka Medical, Inc., Tokyo, Japan).

^{11}C-PBR28 for translocator protein imaging was labeled by ^{11}C-methylation of its *O*-desmethyl precursor with ^{11}C-methyl iodide.[12] Radiochemical purity was >99%, and specific radioactivity was 135.8 ± 38.6 GBq/μmol.

^{11}C-FMZ for CBR was labeled by ^{11}C-methylation of its *N*-desmethyl precursor with ^{11}C-methyl iodide.[13] Radiochemical purity was >99%, and specific radioactivity was 70.0 ± 51.2 GBq/μmol.

The ^{18}F-BCPP-EF was radiolabeled by nucleophilic ^{18}F-fluorination of its corresponding precursor as reported previously.[6] Radiochemical purity was >99%, and specific radioactivity was 139.6 ± 37.0 GBq/μmol.

^{18}F-fluoro-2-deoxy-D-glucose was produced by nucleophilic ^{18}F-fluorination of mannose triflate after basic hydrolysis of 2-^{18}F-fluoro-1,3,4,6-tetra-*O*-acetyl-d-glucose according to a method described previously.[14]

Positron Emission Tomography Analysis in Monkey Brain

After overnight fasting, monkeys were tracheostomized, immobilized with 0.05 mg/kg pancronium bromide intramuscularly every 2 hours, and artificially ventilated. Anesthesia was continued with 0.8% isoflurane in a $N_2O/O_2/N_2$ (1:1:1) gas mixture during the entire experiment. After a transmission scan for 30 minutes using a ^{68}Ge-^{68}Ga rotation rod source, emission scanning with ^{18}F-FDG was conducted for 60 minutes, and scans with ^{11}C-BPR28 and ^{18}F-BCPP-EF were performed for 91 minutes after injection using a high-resolution animal PET scanner (SHR-7700; Hamamatsu Photonics, Hamamatsu, Japan).[15] The PET data obtained were reconstructed by the filtered back projection method with a Hanning filter of 4.5 mm full width at half maximum and attenuation correction using the transmission scan data. Individual PET and MRI images were coregistered. Volumes of interest in brain regions were drawn manually on the MRI referring regional information from BrainMaps.org,[16] and volumes of interest of MRI were superimposed on the coregistered PET images to measure the time-activity curves (TACs) of each PET probe for kinetic analyses. These processes were performed using the PMOD software (PMOD Technologies Ltd., Zurich, Switzerland).

For quantitative analysis of ^{18}F-BCPP-EF, PET scans were conducted with arterial blood sampling as reported previously.[8] Arterial blood samples were obtained every 8 seconds up to 64 seconds, followed by 90, 150 seconds, then 4, 6, 10, 20, 30, 45, 60, and 90 minutes after tracer injection, and these blood samples were centrifuged to separate plasma, weighed, and their radioactivity was measured. For metabolite analysis, methanol was added to some plasma samples (sample/methanol = 1/1) obtained at 16, 40, 64 seconds, 6, 10, 30, and 45 minutes after the injection, followed by centrifugation. The obtained supernatants were developed using thin layer chromatography plates (AL SIL G/UV, Whatman, Kent, UK) with a mobile phase of ethyl acetate. The ratio of unmetabolized fraction was determined using a phosphoimaging plate (FLA-7000; Fuji Film, Tokyo, Japan). The input function of unmetabolized ^{18}F-BCPP-EF was calculated using the data obtained by correction of the ratio of the unmetabolized fraction to total radioactivity, which was used as the arterial input function.

As confirmed in our previous study,[8] kinetic analysis of ^{18}F-BCPP-EF was performed by 2-TC analysis,[17–19] which was performed using the PMOD software (PMOD Technologies Ltd.). The unknown rate constants (K_1, k_2, k_3, and k_4) were calculated to fit the measured tissue radioactivity curve (C_{meas}) in each region of interest (ROI) using the input function, which was the radioactivity curve of the metabolite-corrected arterial plasma. The total distribution volume (V_T) was calculated by $K_1/k_2 \times (1 \pm k_3/k_4)$.

The quantitative analyses of ^{11}C-FMZ and ^{11}C-PBR28 were performed by Logan graphical plot analysis[19] using the PMOD software (PMOD Technologies Ltd.). As an input function, the TAC in the cerebellum or pons was applied instead of the TAC of metabolite-corrected plasma.

Assessments of rCBF, $rCMRO_2$, regional oxygen extraction fraction, and regional cerebral blood volume were conducted using the steady-state ^{15}O-gas inhalation method,[4,5] with the successive inhalation of trace amounts of ^{15}O-CO_2, ^{15}O-O_2, and ^{15}O-CO. The mean values of radioactivity of whole blood and plasma were used for parametric image generation of rCBF, $rCMRO_2$, regional oxygen extraction fraction, and regional cerebral blood volume.[20,21] The CBV correction was performed for rCBF, $rCMRO_2$, and regional oxygen extraction fraction measurements.

During PET measurement with ^{18}F-FDG for 60 minutes, 16 of arterial blood samples were withdrawn for arterial radioactivity measurements. The blood samples obtained at 45 and 60 minutes after injection were also analyzed for blood glucose levels with STAT PROFILE CCX (Nova Biomedical, Waltham, MA, USA). Positron emission tomography images from 40 to 60 minutes after ^{18}F-FDG injection were used to calculate rCMRglc by an autoradiographic method with an operational equation[22] and parameters with lumped constant of 0.56.[23]

Brain Ischemic Model of Monkey

Monkeys were tracheostomized, immobilized with 0.05 mg/kg pancronium bromide intramuscularly every 2 hours, and artificially ventilated (Cato, Drager, Germany). Anesthesia was continued with 0.8% isoflurane in a $N_2O/O_2/N_2$ (1:1:1) gas mixture during the entire experiment. The mean arterial blood pressure, heart rate, rectal temperature, arterial PO_2 and PCO_2, and pH were continuously or regularly monitored. During the experiments, the animal's body temperature was maintained within normal limits with heating blankets. The right MCA was occluded with two microvascular clips *via* a transorbital approach for 3 hours, and then the clips were removed from the MCA for reperfusion.[4,5] Monkeys were allowed to awaken after the scans, and they were subjected to PET measurements with ^{15}O-gases and ^{18}F-BCPP-EF 7 days (Day-7) after 3-hour MCAO ischemic insult. In addition, they were also measured with ^{11}C-FMZ, ^{11}C-PBR28, and ^{18}F-FDG at Day-8.

Regions of interest (ROIs) of inflammatory regions at Day-7 (ROI_{PBR}), defined as areas with >20% increase in ^{11}C-PBR28 binding in the ipsilateral relative to the contralateral hemisphere, were placed on each quantitative image of $rCMRO_2$, ^{11}C-FMZ, ^{18}F-FDG, rCMRglc, and ^{18}F-BCPP-EF. Furthermore, ROIs of infarct regions at Day-7 ($ROI_{Infarct}$), defined as areas with <40% decrease in $rCMRO_2$ in the ipsilateral relative to the contralateral hemisphere as previously reported,[24] were placed on each

quantitative image. The average ROI_{PBR} and $ROI_{Infarct}$ were created from seven animals, and drown on MRI.

Immunohistochemical Assessment

Immunohistochemical assessments were performed with brains sampled at Day-7 after ischemic insults using rabbit anti-Iba1 polyclonal antibody and mouse anti-NeuN monoclonal antibody as reported previously.[5,9] Brains were perfused transcardially with saline, then 4% paraformaldehyde in 0.1 mol/L sodium phosphate (pH 7.4) under anesthesia with overdose sodium pentobarbital. The brains were subsequently removed and postfixed overnight at 4°C in 4% paraformaldehyde, then rapidly frozen in dry ice powder and sliced into 20-μm-thick coronal sections with a cryostat. The sections were mounted on slide glass, and incubated in phosphate buffer saline containing 0.1% Triton X-100 containing 5% normal goat serum for 30 minutesutes and reacted with primary antibodies at 4°C overnight with rabbit anti-Iba1 polyclonal antibody (1:1,000; Wako Pure Chemical Industry, Tokyo, Japan), or mouse anti-NeuN monoclonal antibody (1:500; Millipore). The slides were then washed in phosphate buffer saline containing 0.1% Triton X-100 and incubated with EnVision plus reagents for rabbit or mouse (DAKO) for 30 minutes at room temperature. The sections were treated with 0.02% 3,3′-diaminobenzidine and 0.006% H_2O_2 in 50 mmol/L Tris-HCl buffer (pH 7.6). The slides were finally counterstained with hematoxylin. The brain slides were scanned with NanoZoomer (Hamamatsu Photonics).

Statistical Analysis

Results are expressed as means ± s.d. Comparisons between conditions were performed using the paired, two-tailed Student's *t*-test. A probability level of $<5\%$ ($P<0.05$) was considered to indicate statistical significance.

RESULTS

Aided by individual monkey MRI (Figure 1A), several ROIs were set on PET images of the brain of normal animals to obtain the TACs of ^{18}F-BCPP-EF in each region (Figure 1B, upper panel). The TAC of ^{18}F-BCPP-EF in normal animals peaked at ca. 10 minutes after injection, except for the occipital cortex (peak time = ca. 30 minutes), followed by gradual elimination with time (Figure 2A). The uptake levels at 20 minutes after injection were the highest in the temporal cortex and the striatum, intermediate in the frontal cortex, and the lowest in the occipital cortex, the hippocampus, and the cerebellum in the normal brain (Figure 2A).

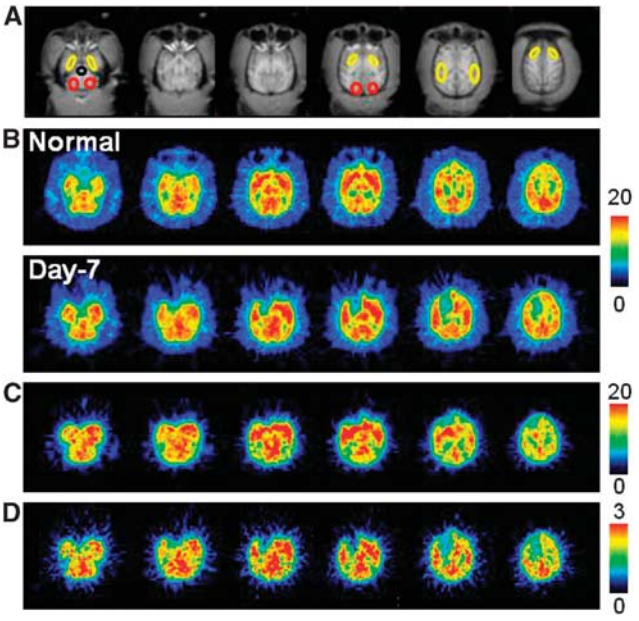

Figure 1. Typical magnetic resonance imaging (MRI) (**A**) and positron emission tomography (PET) images of ^{18}F-BCPP-EF (**B**), regional cerebral blood flow (rCBF) (**C**), and regional cerebral metabolism of oxygen ($rCMRO_2$) (**D**) in the living brain of a monkey (*Macaca fascicularis*). PET images of ^{18}F-BCPP-EF (**B**) were obtained at pre-MCA occlusion ('Normal') and 7 days ('Day-7') postreperfusion after MCA occlusion for 3 hours. PET images of rCBF (**C**) and $rCMRO_2$ (**D**) were obtained at Day-7 only in the same animals as imaged with ^{18}F-BCPP-EF. ^{18}F-BCPP-EF, ^{18}F-2-tert-butyl-4-chloro-5-{6-[2-(2-fluoroethoxy)-ethoxy]-pyridin-3-ylmethoxy}-2H-pyridazin-3-one; MCA, middle cerebral artery.

The kinetics and metabolic rate of ^{18}F-BCPP-EF in the plasma were very rapid; only ca. 6% of nonmetabolized parent compound was detected 90 minutes after the injection (insets of Figures 2A and 2B). Although the chemical species of metabolites have not yet been determined in plasma, they were very polar metabolites unable to enter the brain through the blood–brain barrier. With rapid metabolism of ^{18}F-BCPP-EF, no significant radioactivity accumulation was observed in the skull of monkey, suggesting the minimal defluorination metabolism of ^{18}F-BCPP-EF in plasma and brain tissue (Figure 1B).

As reported previously,[4,5] MCAO of the monkey brain for 3 hours acutely decreased rCBF and $rCMRO_2$ mainly in the striatum, which was the focal area for the supply of blood by the MCA, in the present study (data not shown). At Day-7 after 3-hour MCAO ischemic insult, lower $rCMRO_2$ was detected not only in the striatum, but also in the cortex (Figures 1D and 3B), suggesting the induction of ischemic damage including reperfusion injury in the monkey brain. Our previous results showed that, immediately after reperfusion, postischemic hyperperfusion was observed in the neocortical area of monkey brain.[4,5] In these hyperperfused areas, decreased $rCMRO_2$ was observed thereafter. In contrast, rCBF in the ischemia-damaged area indicated almost the same levels as in the intact area (Figures 1C and 3A).

In the monkey brain after 3-hour MCAO ischemic insult, the TAC of ^{18}F-BCPP-EF also provided a similar TAC pattern as well as uptake levels in the intact side of the brain, showing a peak 10 to 30 minutes after the injection and the uptake levels being the highest in the temporal cortex and the striatum, intermediate in the frontal cortex, and the lowest in the occipital cortex, the hippocampus, and the cerebellum (Figure 2B). In contrast, the TAC in the striatum, and frontal and temporal cortices of the right ischemic hemisphere revealed significantly lower levels than those in the intact hemisphere (Figure 2B). As shown in Figure 1B, the parametric images of V_T of ^{18}F-BCPP-EF were created by 2-TC analysis using the metabolite-corrected plasma input (Figure 2), indicating the reduced binding of ^{18}F-BCPP-EF to MC-I in the damaged brain area of Day-7 after 3 hour MCAO ischemic insult compared with that in the insult area (Figure 3C).

On the PET images of ^{18}F-BCPP-EF (Figure 1B, lower panel), rCBF (Figure 1C), and $rCMRO_2$ (Figure 1D) measured at Day-7 after 3-hour MCAO ischemic insult, the same ROIs, determined with the aid of MRI (Figure 1A), were set on these PET images including both intact and ischemic hemispheres, and then ^{18}F-BCPP-EF data were plotted against rCBF (Figure 4A) or $rCMRO_2$ (Figure 4B). The results showed that the regional V_T of ^{18}F-BCPP-EF did not provide a significant correlation with the rCBF (Figure 4A). In contrast, it should be noted that the regional V_T of both ^{18}F-BCPP-EF was well correlated with the regional $rCMRO_2$ ($R^2=0.720$, $P<0.001$) (Figure 4B).

At Day-7 after 3-hour MCAO ischemic insult, in addition to the ROI-based analyses described above, ROIs of inflammatory regions (ROI_{PBR}), defined as areas with $>20\%$ increase in ^{11}C-PBR28 binding in the ipsilateral relative to the contralateral hemisphere (Figure 5A and red and white colored area in Figure 5F), were placed on each quantitative image of rCMRglc, $rCMRO_2$, ^{11}C-FMZ, and ^{18}F-BCPP-EF (Figures 5B to 5E). The rCMRglc was significantly higher in the ROI_{PBR} of the right ischemic side than that on the corresponding intact side (Figures 5B and 5I). In contrast, ^{18}F-BCPP-EF (Figures 5E and 5I) as well as ^{11}C-FMZ (Figures 5C and 5I) and $rCMRO_2$ (Figures 5D and 5I) was significantly lower in the

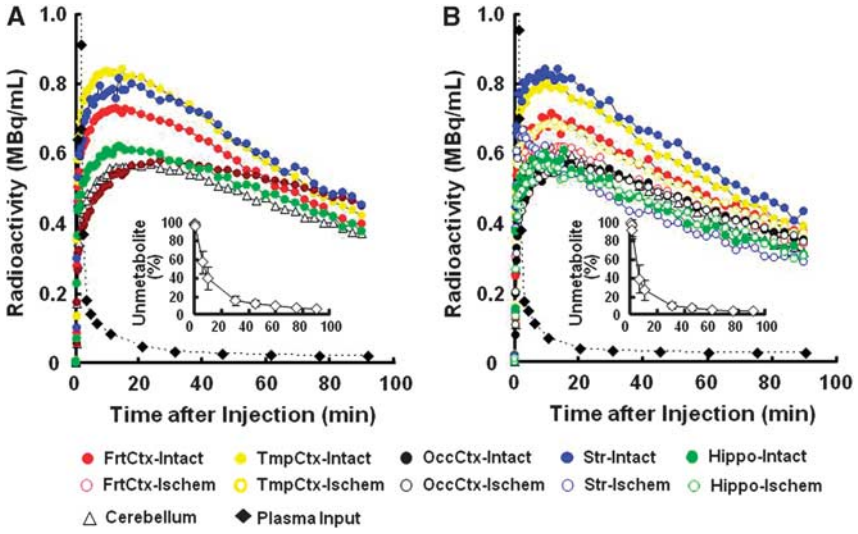

Figure 2. Effects of 3-hour middle cerebral artery (MCA) occlusion (MCAO) ischemic insult on time-activity curves (TACs) of ^{18}F-BCPP-EF in the living brains, metabolite-corrected plasma input, and metabolic profile (insets of **A** and **B**) of monkeys (*Macaca fascicularis*). Before (**A**) and 7 days after the MCA occlusion/reperfusion (**B**), positron emission tomography (PET) scans were conducted for 91 minutes after ^{18}F-BCPP-EF injection, and regions of interest (ROIs) were set on the reconstructed PET images to obtain TACs with the aid of individual magnetic resonance imaging (MRI). Arterial blood samples were sequentially obtained to determine plasma radioactivity curve and metabolic profile. The uptake values in each ROI were normalized to 1 GBq injection dose and 5 kg body weight. TAC data in the brain regions and blood expressed as mean values, and those in metabolic profiles as mean ± s.d. for seven animals. ^{18}F-BCPP-EF, ^{18}F-2-tert-butyl-4-chloro-5-{6-[2-(2-fluoroethoxy)-ethoxy]-pyridin-3-ylmethoxy}-2H-pyridazin-3-one.

ROI_{PBR} of the right ischemic side than on the corresponding intact side. These areas revealed high immunoreactivity to anti-Iba 1 antibody (Figure 5G) and low immunoreactivity to anti-NeuN antibody (Figure 5H).

As shown in Figure 5I, the average $rCMRO_2$ value decreased from 51.8% in ROI_{PBR} to 34.6% in $ROI_{Infarct}$ (white colored area in Figure 5F), which was reasonable because the infarct was determined as $rCMRO_2$ of $<40\%$ of intact side. The V_T ratio of ^{18}F-BCPP-EF also decreased from 58.6% in ROI_{PBR} to 41.0% in $ROI_{Infarct}$, which were well consistent with $rCMRO_2$ alteration. In addition, ^{11}C-FMZ showed lower uptake in $ROI_{Infarct}$ than that in ROI_{PBR}. In contrast, the uptakes of ^{11}C-PBR28 and ^{18}F-FDG showed similar levels both in ROI_{PBR} and in $ROI_{Infarct}$.

DISCUSSION

The present results suggest the potential of ^{18}F-BCPP-EF to be used as a PET probe for the assessment of normal and ischemic impaired MC-I in living brain of nonhuman primate (*Macaca fascicularis*) using PET. All PET measurements in the present study were conducted under isoflurane anesthetic state, since surgical operation of monkeys for MCAO needed some invasive procedures.[4,5] We preliminarily evaluated the effects of isoflurane on ^{18}F-BCPP-EF binding to MC-I by comparing between conscious and anesthetic states in same animals, and concluded that ^{18}F-BCPP-EF binding was not affected by isoflurane anesthesia in the living brain of monkey (Tsukada *et al*, unpublished data). Several reports have suggested that general volatile anesthetics (isoflurane, sevoflurane, and halothane) suppress mitochondrial activity through the inhibition of MC-I, in which the mitochondrial membrane potential ($\Delta\Psi$m) of synaptosomes isolated from rat brain neurons was assessed using fluorescent probes at 1 and 2 minimum alveolar concentration.[25,26] The parameter of $\Delta\Psi$m depends on ATP synthesis, Ca^{2+} sequestration, and ROS production,[27] and is not an exclusive and direct indicator of MC-I activity. In contrast, ^{18}F-BCPP-EF used in the present study is a specific PET probe for measuring the MC-I activity in living brain.[6–8] The dose of isoflurane used in the present study was 0.8 vol.% (0.7 minimum alveolar concentration), which was significantly lower than that used in the previous *in vitro* studies,[25,26] and the actual concentration at mitochondria in the brain should be much lower than 0.7 minimum alveolar concentration by considering the metabolism and the distribution in the living body, resulting in no significant effects on MC-I activity in the living brain as measured by ^{18}F-BCPP-EF.

It has been proposed that an ideal tracer should have high and rapid uptake, rapid washout, followed by reasonably long specific retention in the tissues with the target molecules.[28] From these points of view, the previous[6–8] and present studies suggested that ^{18}F-BCPP-EF could be an ideal PET tracer for MC-I imaging because an appropriate lipophilicity of ^{18}F-BCPP-EF ($logD_{7.4} = 3.03$)[6] could contribute for suitable blood–brain barrier penetration as well as for optimal *in vivo* specific and nonspecific binding ratios for PET probes. In addition, the moderate affinity of ^{18}F-BCPP-EF (Ki = 2.31 nmol/L)[6] resulted in reversible-type kinetics with a pseudo-equilibrium state of radioactivity within the PET scanning time.[6–8] The present results showed that the uptake of ^{18}F-BCPP-EF indicated less rCBF dependence, especially in the regions with luxury perfusion induced after the ischemic neuronal damage in living brain. On the basis of these results, we assumed that K_1/k_2 was the same in all ROIs to obtain a stable result in the present study.

It was confirmed that the uptake of ^{18}F-BCPP-EF reflected the specific binding to cellular MC-I,[7,8] which is the first component of four electron transport complexes in the inner mitochondrial membrane. By *in vitro* assay in rat brain slice, ^{18}F-BCPP-EF binding was inhibited by rotenone, a specific MC-I inhibitor, in a dose-dependent manner.[7] Furthermore, by *in vivo* assay in rat using small animal PET, although dose escalation study was impossible because of the lethal effects of rotenone on cardiac function, the significant reduction in uptake into the brain as well as into the heart was observed even at a relatively low dose of 0.1 mg/kg per hour.[7,8]

^{18}F-fluoro-2-deoxy-D-glucose is useful with easier operation compared with rCBF and $rCMRO_2$ measurements with three consecutive measurements using very short half-life ^{15}O-gases. However, as shown in the present study, higher accumulation of ^{18}F-FDG occurred in both ROI_{PBR} and $ROI_{Infarct}$ than on the

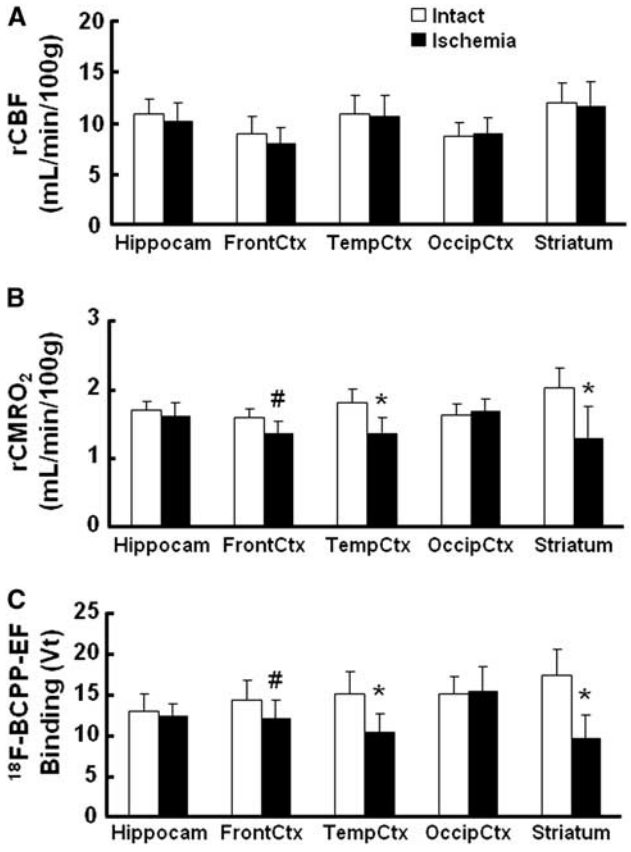

Figure 3. Effects of 3-hour middle cerebral artery occlusion (MCAO) ischemic insult on regional cerebral blood flow (rCBF) (**A**), regional cerebral metabolism of oxygen ($rCMRO_2$) (**B**), and total distribution volume (V_T) of ^{18}F-BCPP-EF (**C**) in the living brains of monkeys (*Macaca fascicularis*). rCBF (**A**) and $rCMRO_2$ (**B**) were determined by three sequential positron emission tomography (PET) measurements with ^{15}O-CO_2, ^{15}O-O_2, and ^{15}O-CO. The V_T values of ^{18}F-BCPP-EF were calculated by 2-TC analysis using time-activity curves (TACs) in cortical regions and metabolite-corrected arterial plasma input (**C**). Regions of interest (ROIs) were set on the hippocampus, striatum, and the frontal, temporal, and occipital cortices in both brain hemispheres with the aid of individual magnetic resonance imaging (MRI). Data are expressed as mean ± s.d. for seven animals. $^{\#}P < 0.05$ vs. each contralateral 'Intact' region. $^{*}P < 0.01$ versus each contralateral 'Intact' region. ^{18}F-BCPP-EF, ^{18}F-2-tert-butyl-4-chloro-5-{6-[2-(2-fluoroethoxy)-ethoxy]-pyridin-3-ylmethoxy}-2H-pyridazin-3-one.

corresponding intact side at Day-7/8 after 3-hour MCAO ischemic insult. Immunohistological study with anti-Iba 1 and anti-NeuN antibodies evidenced that the high ^{18}F-FDG uptake could be attributable to the accumulation of activated microglial cells in ROI_{PBR} and $ROI_{Infarct}$. The higher degrees of ^{18}F-FDG as well as ^{11}C-PBR28 were almost similar in both ROI_{PBR} and $ROI_{Infarct}$ in the present study. The previous reports regarding the relationship between neuronal damage and inflammation indicated controversial results. Some reports showed the increase in ^{11}C-PK-11195 binding in peri-infarct regions, but not in infarct region, at Day-7 in rat ischemic model.[9,10] Another report reported no significant changes in ^{11}C-PK-11195 binding in either peri-infarct or infarct regions at Day-9, similarly increase in both regions Day-21 and later in baboon ischemic model, while ^{11}C-FMZ binding was significantly reduced from Day-2 and later.[29] Take together, the relationship between neuronal damage and inflammation might be altered depending on the species, models and timing after ischemic insult.

In developed cells like neurons, glucose is converted into pyruvate through a tricarboxcylic acid cycle and ultimately produces energy *via* the electron transport system and oxidative phosphorylation, accounting for ca. 85% to 90% of the glucose used in the adult humans.[30] In contrast, activated inflammatory cells, such as macrophages and microglia, produce lactate from glucose, known as the Warburg effect[31] or aerobic glycolysis, accounting for only ca. 5% glucose utilization in oxidative phosphorylation.[30–34] For rCMRglc analyses in this study, we applied a fixed lumped constant of 0.56,[23] which is a correction factor to convert FDG metabolic rate into rCMRglc determined from normal human brains. Since a previous study suggested that rCMRglc calculated with a fixed lumped constant would be underestimated at high metabolic rates and overestimated at low metabolic rates,[35] the rCMRglc in inflammatory (ROI_{PBR}) and infarct ($ROI_{Infarct}$) regions might be underestimated and overestimated. Since recent PET research indicated that several neurodegenerative disorders showed neuroinflammation with microglial activation,[11] based on the metabolic differences between normal neuron cells and activated microglial cells, it could be assumed that MC-I-specific PET probes like ^{18}F-BCPP-EF would be useful as more accurate indicators of neurodegeneration in living brain.

The present results showed that the ischemic-induced infarct areas ($ROI_{Infarct}$), determined as region with $rCMRO_2$ of $<40\%$ of intact side at Day-7 as previously reported,[24] showed much lower V_T of ^{18}F-BCPP-EF than that in ROI_{PBR}. In addition to the inclusion of $ROI_{Infarct}$ in ROI_{PBR}, this result could suggest that inflammatory region includes infarct and peri-infarct regions, which region might be curable remaining high $rCMRO_2$. In these hyperperfused areas, decreased $rCMRO_2$ was observed thereafter, suggesting that reperfusion-related ROS production may in part contribute to neuronal damage of reperfusion injury. Mitochondria are considered the main intracellular source of ROS and also the main target of oxyradical-mediated damage. Since MC-I exhibits lower activity compared with the other respiratory chain complexes, it is a limiting factor in the regulation of oxidative phosphorylation. The decrease in the MC-I activity induced in ischemic/reperfused brain should be associated with a decline in mitochondrial respiration. These factors could reasonably explain the present result of a good correlation between V_T of ^{18}F-BCPP-EF and $rCMRO_2$, which is a conventional indicator of mitochondrial respiration.

It has been reported that ischemic insult induces the diaschisis which is defined as a depression of regional blood flow and metabolism caused by dysfunction in an anatomically separate but functionally related neuronal region, however, may not reflect neuronal death.[36] The present study showed that the V_T of ^{18}F-BCPP-EF was not related to rCBF in the brain (Figure 4A), and also that the V_T of ^{18}F-BCPP-EF was not affected by inflammation (Figures 5E and 5G) that caused high rCMRglc (Figures 5B and 5I). In addition, the decreased V_T of ^{18}F-BCPP-EF was observed in the regions with low immunoreactivity to anti-NeuN antibody (Figures 5E and 5H). Take together, although further studies should be needed, the MC-I imaging using ^{18}F-BCPP-EF might be useful to discriminate diaschisis and neuronal death.

In the present study, ^{11}C-FMZ-PET was also conducted to assess the neural damage in ischemic regions, since CBR was considered to be a superior method for accurate detection of ischemic cerebral damage in primates.[29,37,38] However, since the CBR is exclusively located in the cortex, not in the white matter and basal ganglia, ^{11}C-FMZ can detect the neuronal damage in the cortex. In contrast, ^{18}F-BCPP-EF can image to detect the neuronal damage in whole brain. In addition, the present study showed less ^{11}C-FMZ binding to CBR at Day-7 after 3-hour MCAO cortical ischemic insult than $rCMRO_2$ and ^{18}F-BCPP-EF binding. It was reported that there were no significant changes in the *in vitro* ^{3}H-FMZ binding to CBR in rat brain in the acute phase after 3-hour MCAO cortical ischemic insult.[39] We recently reported a relatively slow temporal change in the rat brain uptake of ^{11}C-FMZ after focal cerebral ischemia after

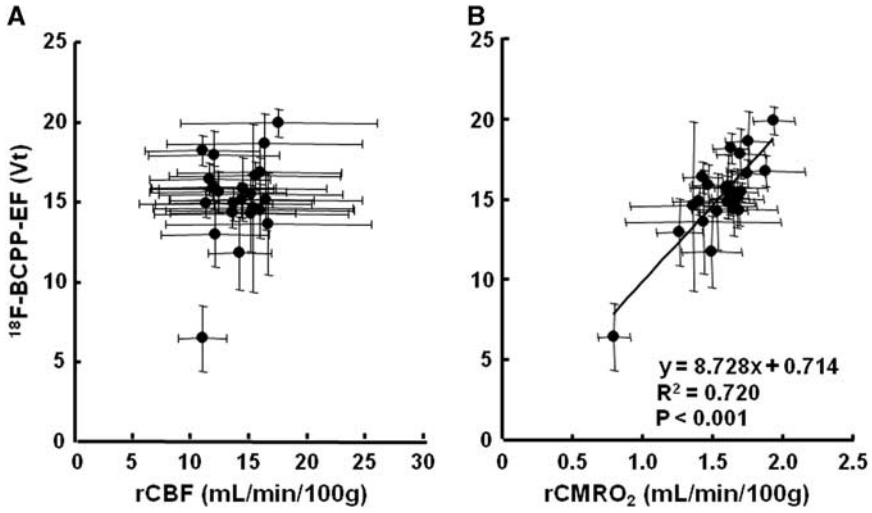

Figure 4. Correlations of total distribution volume (V_T) of ^{18}F-BCPP-EF against regional cerebral blood flow (rCBF) (**A**) and regional cerebral metabolism of oxygen (rCMRO$_2$) (**B**) at Day-7 after 3-hour middle cerebral artery occlusion (MCAO) ischemic insult in the living brains of monkeys (*Macaca fascicularis*). The same regions of interest (ROIs), determined with the aid of individual magnetic resonance imaging (MRI), were set on the positron emission tomography (PET) images of ^{18}F-BCPP-EF, rCBF, and rCMRO$_2$, averaged each ROI across all the monkeys, and then averaged V_T values of ^{18}F-BCPP-EF were plotted against the averaged values of rCBF (**A**) or rCMRO$_2$ (**B**). ^{18}F-BCPP-EF, ^{18}F-2-tert-butyl-4-chloro-5-{6-[2-(2-fluoroethoxy)-ethoxy]-pyridin-3-ylmethoxy}-2H-pyridazin-3-one.

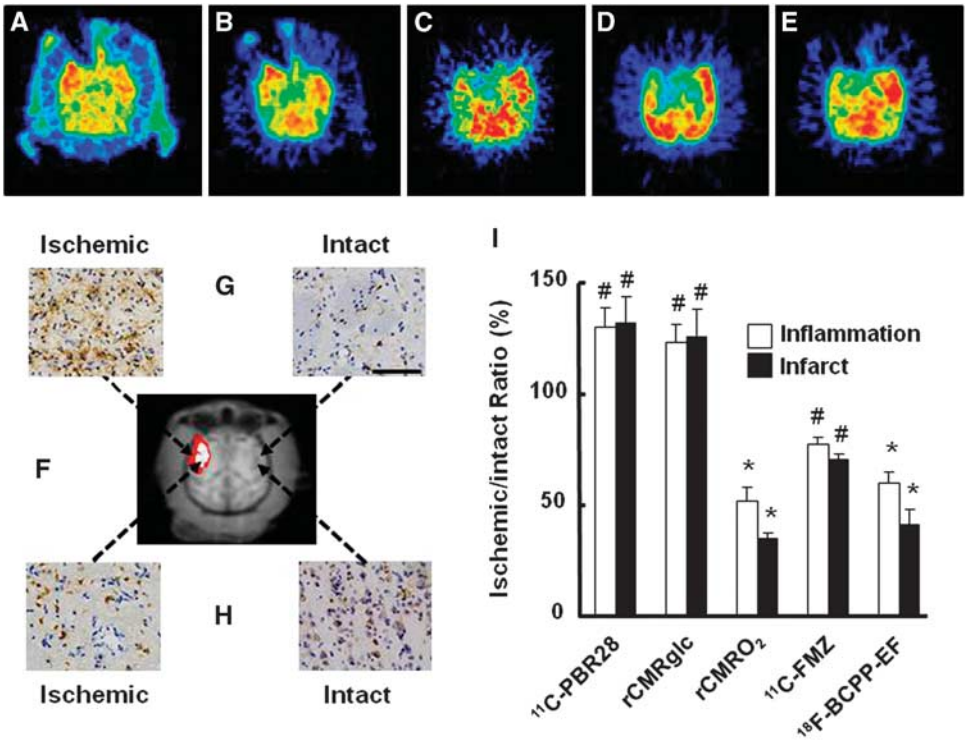

Figure 5. Effects of inflammation with accumulation of activated microglia on ^{11}C-PBR28 binding (**A**), regional cerebral metabolic rate of glucose (rCMRglc) (**B**), regional cerebral metabolism of oxygen (rCMRO$_2$) (**C**), ^{11}C-flumazenil (^{11}C-FMZ) binding (**D**), and ^{18}F-BCPP-EF binding (**E**). Regions of interest (ROIs) of inflammatory (ROI$_{PBR}$) and infarct (ROI$_{Infarct}$) regions at Day-7 (**F**) were placed on each quantitative image of rCMRglc, ^{11}C-FMZ, rCMRO$_2$, and ^{18}F-BCPP-EF, and the ischemic/intact ratios were calculated for each probe (**I**). Data are expressed as mean ± s.d. for seven animals; $^{\#}P < 0.05$, $^{*}P < 0.01$ (**G**). After positron emission tomography (PET) imaging, monkey brains were dissected for immunohistological analyses with anti-Iba 1 (**G**) and anti-NeuN (**H**) antibodies. ^{18}F-BCPP-EF, ^{18}F-2-tert-butyl-4-chloro-5-{6-[2-(2-fluoroethoxy)-ethoxy]-pyridin-3-ylmethoxy}-2H-pyridazin-3-one.

photochemically induced thrombosis.[9] In addition, ^{3}H-FMZ binding *in vivo* was relatively insensitive to cell death induced by sodium nitroprusside, a traditional NO donor compound.[40] These three previous studies and the present data suggest that FMZ binding to CBR might be considerably more stable against cell death, and providing more time to detect neuronal damage in the brain.

One limitation of the present study was that MR imaging could not be conducted after ischemic insult to detect anatomic and pathologic changes because of the Japanese low as described in Materials and methods. If MR imaging data after ischemic insult were coregistered with PET data presented here, then the deeper insight might be obtained for changes in MC-I activity.

In conclusion, the present study succeeded to validate ^{18}F-BCPP-EF, a novel PET probe for MC-I activity, as a specific marker of ischemia-induced neuronal death without being disturbed by inflammation.

DISCLOSURE/CONFLICT OF INTEREST

The authors declare no conflict of interest.

ACKNOWLEDGMENTS

The authors gratefully acknowledge the technical assistance of Aiko Iwazaki, Kaori Suzuki, and Shigeyuki Yamamoto.

REFERENCES

1 Kroemer G, Reed JC. Mitochondrial control of cell death. *Nat Med* 2000; **6**: 513–519.
2 Perez-Pinzon MA, Stetler RA, Fiskum G. Novel mitochondrial targets for neuroprotection. *J Cereb Blood Flow Metab* 2012; **32**: 1362–1376.
3 Schild L, Huppelsberg J, Kahlert S, Keilhoff G, Reiser G. Brain mitochondria are primed by moderate Ca^{2+} rise upon hypoxia/reoxygenation for functional breakdown and morphological disintegration. *J Biol Chem* 2003; **278**: 25454–25460.
4 Takamatsu H, Tsukada H, Kakiuchi T, Nishiyama S, Noda A, Umemura K. Detection of reperfusion injury using positron emission tomography in a monkey model of cerebral ischemia. *J Nucl Med* 2000; **41**: 1409–1416.
5 Tsukada H, Fukumoto D, Nishiyama S, Sato K, Kakiuchi T. Transient focal ischemia affects the cAMP second messenger system and coupled dopamine D1 and 5-HT1A receptors in the living monkey brain: a PET study using microdialysis. *J Cereb Blood Flow Metab* 2004; **24**: 898–906.
6 Harada N, Nishiyama S, Kanazawa M, Tsukada H. Development of novel PET probes, [18F]BCPP-EF, [18F]BCPP-BF, and [11C]BCPP-EM for mitochondrial complex I imaging in the living brain. *J Labeled Comp Radiopharm* 2013; **56**: 553–561.
7 Tsukada H, Nishiyama S, Fukumoto D, Kanazawa M, Harada N. Novel PET probes 18F-BCPP-EF and 18F-BCPP-BF for mitochondrial complex I: a PET study by comparison with 18F-BMS-747158-02 in rat brain. *J Nucl Med* 2014; doi:10.2967/jnumed.113.125328 (in press).
8 Tsukada H, Ohba H, Kanazawa M, Kakiuchi T, Harada N. Evaluation of 18F-BCPP-EF for mitochondrial complex 1 imaging in conscious monkey brain using PET. *Eur J Nucl Med Mol Imaging* 2013; doi:10.1007/s00259-013-2628-z (in press).
9 Fukumoto D, Hosoya T, Nishiyama S, Harada N, Iwata H, Yamamoto S *et al.* Multiparametric assessment of acute and sub-acute ischemic neuronal damage: a small animal PET study with rat photochemically induced thrombosis (PIT) model. *Synapse* 2011; **65**: 207–214.
10 Schroeter M, Dennin MA, Walberer M, Backes H, Neumaier B, Fink GR *et al.* Neuroinflammation extends brain tissue at risk to vital peri-infarct tissue: a double tracer [11C]PK11195- and [18F]FDG-PET study. *J Cereb Blood Flow Metab* 2009; **29**: 1216–1225.
11 Winkeler A, Boisgard R, Martin A, Tavitian B. Radioisotopic imaging of neuroinflammation. *J Nucl Med.* 2010; **51**: 1–4.
12 Briard E, Zoghbi SS, Imaizumi M, Gourley JP, Shetty HU, Hong J *et al.* Synthesis and evaluation in monkey of two sensitive 11C-labeled aryloxyanilide ligands for imaging brain peripheral benzodiazepine receptors in vivo. *J Med Chem* 2008; **51**: 17–30.
13 Maziere M, Hantraye P, Prenant C, Sastre J, Comar D. Rol5 1788, a specific radioligand for 'in vivo' central benzodiazepine receptor study by positron emission tomography. *Appl Radiat Isot* 1984; **35**: 973–976.
14 Oberdorfer F, Hull WE, Traving BC, Maier-Borst W. Synthesis and purification of 2-deoxy-2-18fluoro-D-glucose and 2-deoxy-2-18fluoro-D-mannose: characterization of products by 1H and 19F-NMR spectroscopy. *Int J Rad Appl Instrum A* 1986; **37**: 695–700.
15 Watanabe M, Okada H, Shimizu K, Omura T, Yoshikawa E, Kosugi T *et al.* A high resolution animal PET scanner using compact PS-PMT detectors. *IEEE Trans Nucl Sci* 1997; **44**: 1277–1282.
16 Jones EG, Stone JM, Karten HJ. High-resolution digital brain atlases: a Hubble telescope for the brain. *Ann NY Acad Sci* 2011; **1225 S1**: E147–E159.
17 Huang SH, Barrio J, Phelps M. Neuroreceptor assay with positron emission tomography; equilibrium versus dynamic approach. *J Cereb Blood Flow Metab* 1986; **6**: 515–521.
18 Mintun MA, Raichle ME, Kilbourn MR, Wooten GF, Welch MJ. A quantitative model for the in vivo assessment of drug binding sites with positron emission tomography. *Ann Neurol* 1984; **15**: 217–227.
19 Logan J, Fowler JS, Volkow ND, Wolf AP, Dewey SL, Schlyer DJ *et al.* Graphical analysis of reversible radioligand binding from time-activity measurements applied to [N-11C-methyl]-(-)-cocaine PET studies in human subjects. *J Cereb Blood Flow Metab* 1990; **10**: 740–747.
20 Frackowiak RSJ, Lenzi GL, Jones T, Hearther JD. Quantitative measurement of regional cerebral blood flow and oxygen metabolism in man using 15O and positron emission tomography: theory, procedure and normal values. *J Comput Assist Tomogr* 1980; **4**: 727–736.
21 Touzani O, Young AR, Derlon J-M, Beaudouin V, Marchal G, Rioux P *et al.* Sequential studies of severely hypometabolic tissue volumes after permanent middle cerebral artery occlusion. A positron emission tomographic investigation in anesthetized baboons. *Stroke* 1995; **26**: 2112–2119.
22 Sokoloff L, Reivich M, Kennedy C, Des Rosiers MH, Patlak CS, Pettigrew KD *et al.* The [14C]deoxyglucose method for the measurement of local cerebral glucose utilization: theory, procedure, and normal values in the conscious and anesthetized albino rat. *J Neurochem* 1977; **28**: 897–916.
23 Reivich M, Alavi A, Wolf A, Fowler J, Russell J, Arnett C *et al.* Glucose metabolic rate kinetic model parameter determination in humans: the lumped constants and rate constants for [18F]fluorodeoxyglucose and [11C]deoxyglucose. *J Cereb Blood Flow Metab* 1985; **5**: 179–192.
24 Touzani O, Young AR, Derlon JM, Baron JC, MacKenzie ET. Progressive impairment of brain oxidative metabolism reversed by reperfusion following middle cerebral artery occlusion in anaesthetized baboons. *Brain Res* 1997; **767**: 17–25.
25 Hanley PJ, Ray J, Brandt U, Daut J. Halothane, isoflurane and sevoflurane inhibit NADH:ubiquinone oxidoreductase (complex I) of cardiac mitochondria. *J Physiol* 2002; **544**: 687–693.
26 Moe MC, Bains R, Vinje ML, Larsen GA, Kampenhang EB, Berg-Johnsen J. Sevoflurane depolarizes pre-synaptic mitochondria in the central nervous system. *Acta Anaesthesiol Scand* 2004; **48**: 562–568.
27 Nicholls DG, Budd SL. Mitochondria and neuronal survival. *Physiol Rev* 2000; **80**: 315–360.
28 Waterhouse RN. Determination of lipophilicity and its use as a predictor of blood-brain barrier penetration of molecular imaging agents. *Mol Imaging Biol* 2003; **5**: 376–389.
29 Sette G, Baron JC, Young AR, Miyazawa H, Tillet I, Barre L *et al.* In vivo mapping of brain benzodiazepine receptor changes by positron emission tomography after focal ischemia in the anesthetized baboon. *Stroke* 1993; **24**: 2046–2058.
30 Vander Heiden MG, Cantley LC, Thompson CB. Understanding the Warburg effect: the metabolic requirements of cell proliferation. *Science* 2009; **324**: 1029–1033.
31 Warburg O. On respiratory impairment in cancer cells. *Science* 1956; **124**: 269–270.
32 Radu CG, Shu CJ, Shelly SM, Phelps ME, Witte ON. Positron emission tomography with computed tomography imaging of neuroinflammation in experimental autoimmune encephalomyelitis. *Proc Natl Acad Sci USA* 2007; **104**: 1937–1942.
33 Maciver NJ, Jacobs SR, Wieman HL, Wofford JA, Coloff JL, Rathmell JC. Glucose metabolism in lymphocytes is a regulated process with significant effects on immune cell function and survival. *J Leukoc Biol* 2008; **84**: 949–957.
34 Garedew A, Henderson SO, Moncada S. Activated macrophages utilize glycolytic ATP to maintain mitochondrial membrane potential and prevent apoptotic cell death. *Cell Death Differ* 2010; **17**: 1540–1550.
35 Gjedde A, Wienhard K, Heiss WD, Kloster G, Diemer NH, Herholz K *et al.* Comparative regional analysis of 2-fluorodeoxyglucose and methylglucose uptake in brain of four stroke patients. With special reference to the regional estimation of the lumped constant. *J Cereb Blood Flow Metab* 1985; **5**: 163–178.
36 Feeney DM, Baron JC. Diaschisis. *Stroke* 1986; **17**: 817–830.
37 Heiss WD, Kracht L, Grond M, Rudolf J, Bauer B, Wienhard K *et al.* Early [11C]flumazenil/H_2O positron emission tomography predicts irreversible ischemic cortical damage in stroke patients receiving acute thrombolytic therapy. *Stroke* 2000; **31**: 366–369.
38 Zhao L, Yamashima T, Wang X-D, Tonchev AB, Yamashita J, Kakiuchi T *et al.* PET imaging of ischemic neuronal death in the hippocampus of living monkey. *Hippocampus* 2001; **12**: 309–318.
39 Abe K, Kashiwagi Y, Tokumura M, Hosoi R, Hatazawa J, Inoue O. Discrepancy between cell injury and benzodiazepine receptor binding after transient middle cerebral artery occlusion in rats. *Synapse* 2004; **53**: 234–239.
40 Inoue O, Yanamoto K, Fujiwara Y, Hosoi R, Kobayashi K, Tsukada H. Sensitivities of benzodiazepine receptor binding and muscarinic acetylcholine receptor binding for the detection of neural cell death caused by sodium nitroprusside microinjection in rat brain. *Synapse* 2003; **49**: 134–141.